Available online at www.sciencedirect.com
SCIENCE DIRECT®
Pergamon
Cement and Concrete Research 34 (2004) 463–480
CEMENT AND CONCRETE RESEARCH

Prediction of diffusivity of concrete based on simple analytic equations

Byung Hwan Oh[a,*], Seung Yup Jang[b]

[a]Department of Civil Engineering, Seoul National University, San 56-1, Shinrim-dong, Gwanak-ku, Seoul 151-742, Republic of Korea
[b]Track and Civil Engineering Research Department, Korea Railroad Research Institute, 360-1, Woulam-dong, Uiwang, Kyounggi-do 437-050, Republic of Korea

Received 5 February 2003; accepted 29 August 2003

Abstract

Proposed is a simple analytic model that can predict realistically the diffusivities of concrete and mortar. The basic concept of the model comes from the relation between the diffusivities and the microstructure of concrete. The microstructure that affects the diffusivity includes the interfacial transition zone (ITZ) between aggregates and cement pastes as well as the microstructure of cement paste itself. The general effective media (GEM) equation was introduced to derive the diffusivity of cement paste. The effective diffusivity of concrete is derived on the basis of the composite sphere assemblage model, which considers the diffusivities of both ITZ and cement paste. The main parameters in the proposed model are the microstructural properties of cement paste such as capillary porosity and pore structure parameter, solid phase diffusivity, aggregate volume fraction, and interfacial zone properties. To validate the proposed model, many series of concrete and mortar specimens have been tested to measure the diffusivities. The major test variables include the water-to-binder ratios, the types and amount of mineral admixtures on the diffusivities. The effects of compressive strength, water-to-binder ratio, and mineral admixtures have been investigated comprehensively. The comparison of the proposed theory with the test data exhibits reasonably good correlation. The proposed model allows more accurate prediction of diffusion process and, thus, more realistic durability design of concrete structures.

Keywords: Concrete; Diffusion; Durability; Interfacial transition zone (ITZ); Microstructure

1. Introduction

Recently, it is increasingly recognized that the strength-based design alone cannot ensure the long and durable service life of concrete structures. Therefore, it is necessary that the durability should be one of the major components in the rational design of concrete structures. In the durability design, one of the most important factors that determine the service life of structures is the transport property of concrete; e.g., the diffusivity of ions and gases. However, it is very difficult to predict the diffusivity of concrete realistically because the concrete diffusivity is influenced by many parameters such as the interfacial zone property between aggregate particles and bulk cement paste as well as the microstructure of the cement paste itself (porosity and pore structure). Moreover, the standard test methods for the diffusivity of concrete have not been established yet, mainly due to the difficulties of the measurement.

On the other hand, the realistic model for the diffusivity of concrete must take into account important influencing variables, yet simple enough for practical application in durability design.

The purpose of this study is, therefore, to propose a simple analytic model to estimate the diffusivity of concrete considering various important factors. The relationship between the diffusivity and the structure of concrete, i.e., the interfacial transition zone (ITZ) between the aggregate particles and the bulk cement paste as well as the microstructure of the bulk cement paste itself are considered to derive the analytic model. Many series of concrete and mortar specimens were tested to verify the proposed model on the diffusivities.

2. Model for diffusivities

2.1. Structure of concrete

The diffusivity of a porous material is strongly dependent on its microstructure such as the tortuosity and interconnectivity of the pore system. Furthermore, the structure of

* Corresponding author. Tel.: +82-2-880-7350; fax: +82-2-887-0349.
E-mail address: bhohcon@snu.ac.kr (B.H. Oh).

0008-8846/$ – see front matter © 2004 Elsevier Ltd. All rights reserved.
doi:10.1016/j.cemconres.2003.08.026

concrete is highly heterogeneous and complex than any other porous materials in that the sizes of aggregate particles and hydrated solid components in concrete vary in very wide range from nanometers to centimeters. In the viewpoint of modeling, concrete is often described as a three-phase composite (Fig. 1). The first and second phases are the cement paste and the aggregate particles, respectively. The third phase is the interface between the aggregate particles and the surrounding cement paste, called "interfacial transition zone (ITZ)." The ITZ is of great importance because it is a "zone of weakness" in the microstructure of concrete, in terms of transport properties as well as in terms of strength [1]. Hence, to predict accurately the transport properties of concrete, the ITZ should be taken into account correctly.

As depicted in Fig. 1, the bulk cement paste itself also can be regarded as a two-phase composite; the first phase is the capillary pore phase, and the second is the solid phase consisting of various hydration products. It should be noted that the C-S-H gel pores are included in the solid phase, not in the pore phase. The main path of transport in hardened cement paste is known to be the capillary pore space while the gel pores play a minor role in transport [1], except at very low capillary porosity.

2.2. Effective diffusivity of cement paste: application of general effective media equation

The effective diffusivity and the conductivity of a porous material can be expressed by the following relationship with pore structure parameter [2].

$$\frac{D_p}{D_0} = \frac{\sigma_p}{\sigma_0} = \phi_{cap}\beta \tag{1}$$

where D_p and σ_p are the effective diffusivity [m^2/s] and the conductivity [$1/\Omega\cdot m$] of the porous material, respectively, when it is regarded as an effective medium. D_0 and σ_0 are the diffusivity and conductivity in a continuum [m^2/s], e.g., ionic diffusivity (or conductivity) in bulk water, ϕ_{cap} is the capillary porosity (–) and β is the pore structure parameter (–). The diffusion paths in the porous medium are tortuous according to the pore structure, and constricted or disconnected at a certain point by nonuniform cross-sectional area of pores [3] [see also Fig. 2]. These characteristics of diffusion in the porous medium are reflected by the pore structure parameter β, which can be defined as $\beta = \delta/\tau^2$ where τ is the tortuosity and δ is the constrictivity of the pore network [5]. The capillary porosity ϕ_{cap} represents the fraction of the cross-sectional area on any given plane, taken from the material, that diffusion can take place. In the above equation, the relationship $\sigma_p/\sigma_0 = D_p/D_0$ is also given by the Nernst–Einstein relation [6].

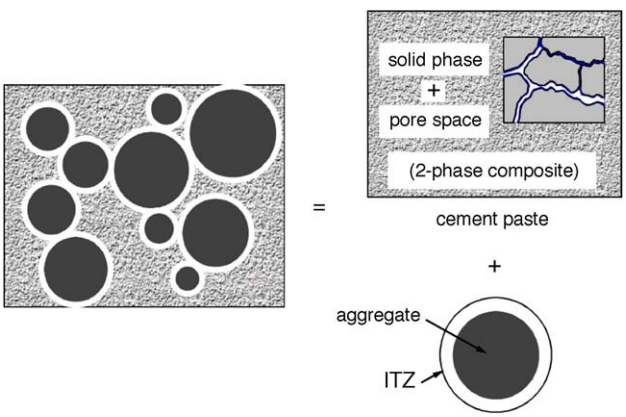

Fig. 1. Structure of concrete.

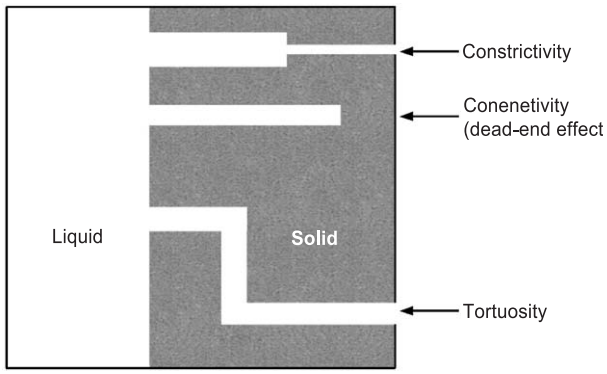

Fig. 2. Schematic of constrictivity, connectivity and tortuosity of a pore network (after Shane et al. [4]).

General composite theories can be used to quantify the "pore structure parameter." The simplest one is probably Archie's law [7], which is expressed as

$$\sigma_p = a \cdot \phi_{cap}^n. \tag{2}$$

The effective medium theory, e.g., Bruggeman asymmetric medium theory, also gives the similar form of relation to Eq. (2) [8]. According to Bruggeman asymmetric equation, when the conductivity of the dispersion medium is perfectly insulated, the empirical constant a corresponds to σ_0, since $\sigma_p = \sigma_0$ when $\phi_{cap} = 1$. The exponent n can be obtained theoretically from the morphology and distribution of the conductors in the mixture of conductors and insulators. Similarly, in the porous medium, the exponent n is determined by the constrictivity and tortuosity of the pore network.

Moreover, considering the percolation of the entire pore network, the following equation, which takes into account the critical porosity, ϕ_c, is more appropriate than Eq. (2) [8].

$$\frac{\sigma_p}{\sigma_0} = \left(\frac{\phi_{cap} - \phi_c}{1 - \phi_c}\right)^n \tag{3}$$

where the percolation threshold ϕ_c is the critical porosity that the pore network first percolates and n is called the

percolation exponent. This equation implies that the conduction or diffusion can occur, only over the percolation threshold. Then, $(\phi_{cap} - \phi_c)$ represents the fraction of open capillary porosity. Bentz and Garboczi [9] have found that the percolation threshold of cement paste, with or without pozzolanic material addition, is about 0.18 from the numerical simulation using their three-dimensional image-based hydration model. They also argue that this percolation threshold is in reasonable agreement with the "universal" value 0.16 [10] for the materials being composed of random nonoverlapping spheres. Recently, the model percolation results have been updated to $\phi_c = 0.17$ [11]. Also, it is found that the value of n is in the range of 1.65 to 2.0, yet higher n values are often encountered in practice when the conducting phases have extreme geometries [8].

Unlike other porous materials, however, the solid phase of the cement paste has also pores, i.e., C-S-H gel pores, and hence, is also diffusive [12]. This means that even if the capillary porosity is less than the percolation threshold, the diffusion can occur. According to the effective medium equation and percolation theory, the conductivity below the percolation threshold can be given as [8]

$$\frac{\sigma_p}{\sigma_s} = \left(1 - \frac{\phi_{cap}}{\phi_c}\right)^{-n} \tag{4}$$

in which σ_s is the conductivity of the low conductance phase [1/Ω·m], i.e., the solid phase of cement paste in this case.

However, the biggest problem in percolation equations, Eqs. (3) and (4), is that they cannot allow the prediction of the conductivity near the percolation threshold because the conductivity given by Eq. (3) approaches zero as $\phi_{cap} \to \phi_c$ while Eq. (4) yields infinity at $\phi_{cap} = \phi_c$ [see Fig. 3]. This shortcoming can be overcome by introducing the general effective media (GEM) equation [8], which is given as

$$\frac{(1-\phi_{cap})(\sigma_s^{1/n} - \sigma^{1/n})}{\sigma_s^{1/n} + A_c\sigma^{1/n}} + \frac{\phi_{cap}(\sigma_0^{1/n} - \sigma^{1/n})}{\sigma_0^{1/n} + A_c\sigma^{1/n}} = 0 \tag{5}$$

where $A_c = (1-\phi_c)/\phi_c$. The above equation is able to account for a nonzero solid phase conductivity (or diffusivity) problem, and allows the prediction of the conductivity even near the percolation threshold. Therefore, this equation is more suitable for predicting the diffusivity of hydrated cement paste considering the characteristics of its microstructure.

From the Nernst–Einstein relation [6], $\sigma_p/\sigma_0 = D_p/D_0$ and $\sigma_s/\sigma_0 = D_s/D_0$. Then, the analytic solution to the above GEM equation can be derived in terms of the normalized diffusivities as follows [13].

$$\frac{D_p}{D_0} = \left(m_\phi + \sqrt{m_\phi^2 + \frac{\phi_c}{1-\phi_c}\left(\frac{D_s}{D_0}\right)^{1/n}}\right)^n \tag{6a}$$

by defining

$$m_\phi = \frac{1}{2}\left[\left(\frac{D_s}{D_0}\right)^{1/n} + \frac{\phi_{cap}}{1-\phi_c}\left(1 - \left(\frac{D_s}{D_0}\right)^{1/n}\right) - \frac{\phi_c}{1-\phi_c}\right] \tag{6b}$$

where D_s/D_0 is the normalized diffusivity of the solid phase (−), which denotes the diffusivity when the

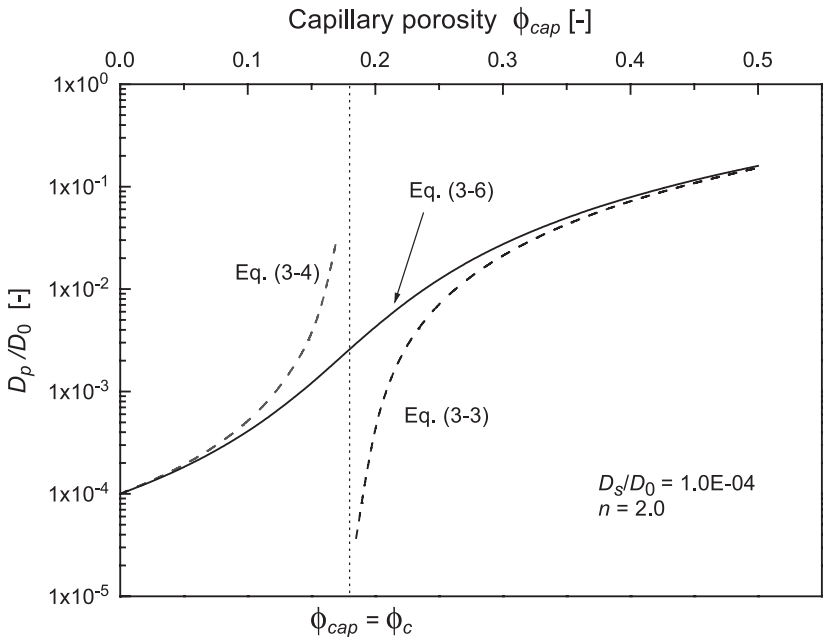

Fig. 3. Conductivity versus capillary porosity based on classical GEM equation (after McLachlan et al. [8]).

capillary porosity equals to zero, and depends on the complexity of the structure of hydrated solid matrix. It is noted here that Eqs. (6a) and (6b) reduces to Eq. (3), when $D_s/D_0 = 0$.

The above equation for diffusivity of cement paste has been compared with the test data available in the literature on the diffusivities of ordinary cement pastes and silica fumed cement pastes. Fig. 4 shows that Eqs. (6a) and (6b) is in reasonable agreement with experimental data found in the literature [14–18]. It was also found that there exist some constant values of n and D_s/D_0 in Eqs. (6a) and (6b) for each type of cement paste. The realistic values for n and D_s/D_0 obtained from the test data are $n \approx 2.7$ and $D_s/D_0 \approx 2.0 \times 10^{-4}$ for Portland cement pastes, and $n \approx 4.5$ and $D_s/D_0 \approx 5.0 \times 10^{-5}$ for silica fume pastes, respectively. It is interesting to note that the value of percolation exponent is higher for the case of the cement paste with silica fume. This may be explained by the refinement of the pore structure by the pozzolanic reaction of silica fume [16], which is supported by several mercury intrusion porosimetry (MIP) data that can be found in Refs. [19,20].

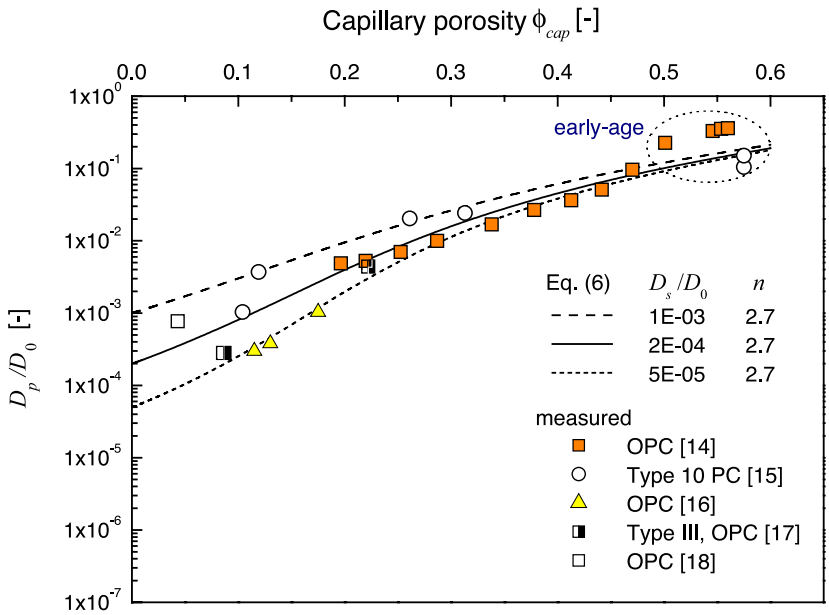

(a) Portland cement pastes

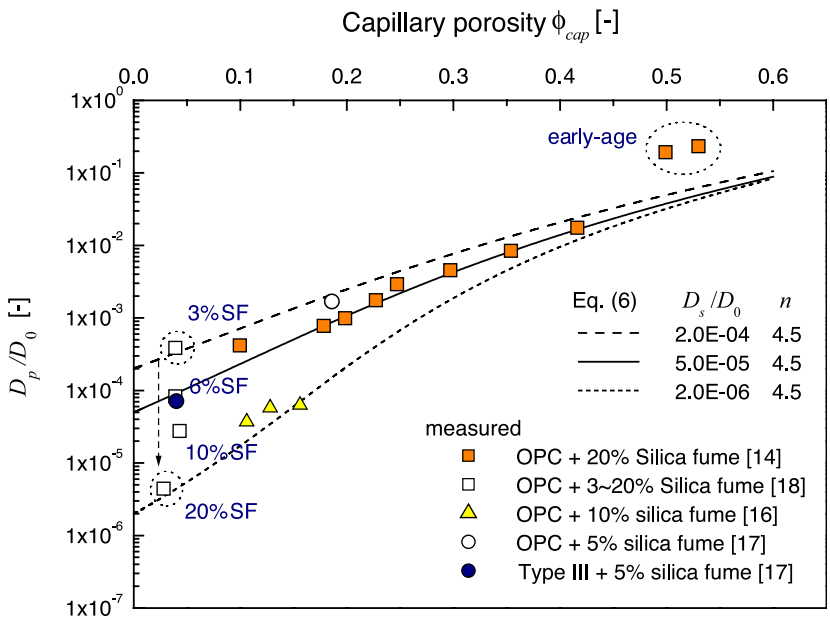

(b) Silica fume pastes

Fig. 4. Comparison predicted diffusivities by GEM equation with measured diffusivities of cement pastes.

The values of D_s/D_0 vary in rather wide range (from 2.0×10^{-6} to 1×10^{-3}) and decrease with increasing amount of silica fume addition (see Fig. 4). This indicates that the pozzolanic C-S-H gel has finer gel pores and thus more intricate pore structure than Portland cement pastes. Hence, the more pozzolans is used, the less D_s/D_0 will be achieved. Bentz et al. [11] also calculated D_s/D_0 to be 4.0×10^{-4}, 3.0×10^{-4}, 1.0×10^{-4} and 1.0×10^{-5} for the Portland cement pastes containing 0, 3, 6 and 10% silica fume, respectively. Although these D_s/D_0 values are slightly larger than the present results, the decreasing patterns of D_s/D_0 according to the amount of silica fume are quite similar.

As compared with the conventional range of the percolation exponent, 1.65–2.0, the value of n for cement pastes are rather higher. From this, it is inferred that the microstructure of the well-hydrated cement paste may be more complex than that of other conventional composites.

2.3. Diffusivity of concrete: application of composite spheres assemblage (CSA) model

Garboczi and Bentz [21] proposed a comprehensive multiscale model to predict the diffusivity of concrete considering the ITZ. They calculated the volume of the ITZ assuming that the thickness of ITZ is constant regardless of the dimension of aggregate particles, and developed the relationship between the diffusivity of cement paste and that of concrete based on the effective medium theory. Actually, the ITZ does not have sharp interfaces with cement paste matrix, nor is uniform. Nevertheless, only for the sake of modeling, the ITZ is considered as a uniform region that has a certain thickness.

On the other hand, the effect of the ITZ on the diffusion coefficients of concrete also can be taken into account by means of a much simpler analytic model than Garboczi and Bentz's [21]. It is the "composite spheres assemblage (CSA)" model proposed originally by Hashin [22]. Hashin has recently developed a model for the conduction in a composite with the imperfect interfaces between matrix and particle inclusions. When this model is applied to a composite spheres assemblage, the conductivity can be written as

$$\frac{\sigma}{\sigma_p}=1+\frac{V_a}{\dfrac{1}{(\sigma_{EH}/\sigma_p)-1}+\dfrac{1-V_a}{3}} \tag{7a}$$

where σ_{EH} is the conductivity of the "effective homogeneous (EH)" composite phase consisting of the aggregate particle and the interface, i.e.,

$$\frac{\sigma_{EH}}{\sigma_p}=\frac{1-2[1-(\sigma_i/\sigma_a)\varepsilon]}{1+(\sigma_a/\sigma_i)\varepsilon}\frac{\sigma_a}{\sigma_p} \tag{7b}$$

in which V_a is the volume fraction of aggregate particle inclusions (−), $\varepsilon=t_i/r_a$ (−) is the ratio of the interface thickness (t_i) and the radius of aggregate particle inclusion (r_a), and σ, σ_p and σ_i are the conductivities of the entire effective medium, of the matrix, and of the interface, respectively. Actually, Eqs. (7a) and (7b) reduce to a lower bound of the conductivity when $\varepsilon=0$, which is well known as Hashin–Shtrikman lower bound [23]. However, the conductivity becomes higher than this bound as ε increases.

The disadvantage of the CSA model is that the equation is derived based on the assumption that ε is always constant, which means that the thickness of ITZ is proportional to the radius of aggregate particle. This is not realistic and it seems rather practical to assume that the interface thickness is same for all particles as Garboczi and Bentz [21] do. Hashin [22] proposes that Eqs. (7a) and (7b) are also applicable to that case by considering the average intensity in any particle, which can be estimated by embedding a composite sphere consisting of a spherical particle and concentric particle/matrix volume fractions in an effective material as in the whole composite (see Fig. 5) [24]. This approximate method is known as general self-consistent scheme (GSCS) [22]. In this case, the spherical particle is EH with conductivity of Eq. (7a). Thus, according to this basic context in GSCS, the conductivity of the CSA with constant interface thickness can be approximately obtained from Eqs. (7a) and (7b) by considering the average flow to a spherical particle with average radius $\bar{r}_a$ as described in Fig. 5.

The conductivity of Eqs. (7a) and (7b) can be replaced by the diffusivity from the Nernst–Einstein relation [6]. If the

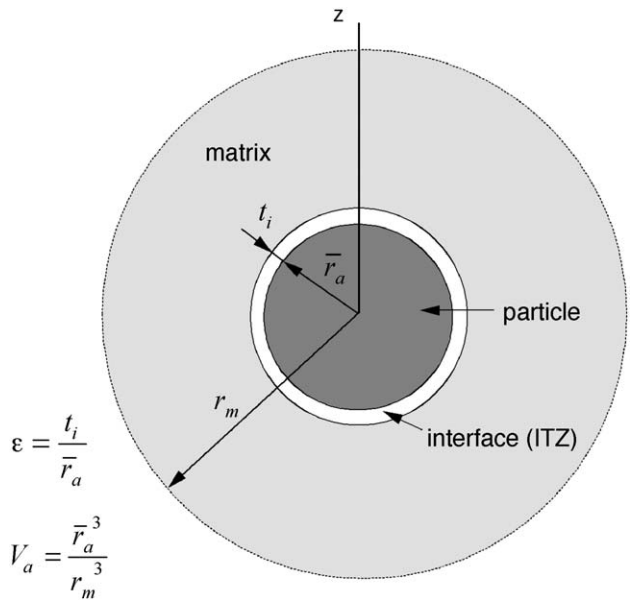

Fig. 5. Conceptual diagram of a composite sphere consisting of a particle and concentric particle/matrix volume fractions for GSCS (after Hashin and Monteiro [24]).

diffusivity of aggregate particle inclusions is assumed zero, i.e., $D_a = 0$, then Eqs. (7a) and (7b) reduces to

$$\frac{D}{D_p} = 1 + \frac{V_a}{\dfrac{1}{2(D_i/D_p)\varepsilon - 1} + \dfrac{1 - V_a}{3}}. \quad (8)$$

The diffusivities of cement paste (D_p) and ITZ (D_i) can be calculated if the porosities are known. Then, from Eq. (8), it is obvious that the diffusivity of concrete, D, is determined by the aggregate volume fraction (V_a), the diffusivity of the ITZ relative to that of cement paste (D_i/D_p), and the thickness ratio of the ITZ (ε). The relationship between the diffusivity of concrete D and the aggregate volume fraction V_a is demonstrated in Fig. 6 for various $(D_i/D_p)\varepsilon$.

2.4. Summary of model

As a consequence, according to the model proposed in the above, the effective diffusivity of concrete or mortar can be written as

$$D = D_0 \cdot \Delta_\phi \cdot \Delta_a \quad (9)$$

where Δ_ϕ is given by Eqs. (6a) and (6b) as

$$\Delta_\phi(\phi_{cap}; D_s/D_0, n) = \left[0.5[(D_s/D_0)^{1/n} + 1.22\phi_{cap}\{1 - (D_s/D_0)^{1/n}\} - 0.22] + \sqrt{0.25[(D_s/D_0)^{1/n} + 1.22\phi_{cap}\{1-(D_s/D_0)^{1/n}\} - 0.22]^2 + 0.22(D_s/D_0)^{1/n}}\right]^n$$

and Δ_a is given by Eq. (8) as

$$\Delta_a(V_a; D_i/D_p, \varepsilon) = 1 + \frac{V_a}{\dfrac{1}{2(D_i/D_p)\varepsilon - 1} + \dfrac{1 - V_a}{3}}.$$

The percolation exponent ϕ_c is taken here as 0.18, as proposed by Bentz and Garboczi [9], and $D_0 = 2.032 \times 10^{-9}$ m^2/s at 25 °C for chloride ions [25]. As can be seen in the above equation, the concrete diffusivity is determined by two main variables, i.e., the capillary porosity ϕ_{cap} and the aggregate volume fraction V_a, and the main parameters of the model are the normalized solid phase diffusivity D_s/D_0, the percolation exponent n, the ratio of the ITZ diffusivity to the diffusivity of bulk cement paste D_i/D_p, and the thickness of ITZ relative to the average radius of aggregate particles ε.

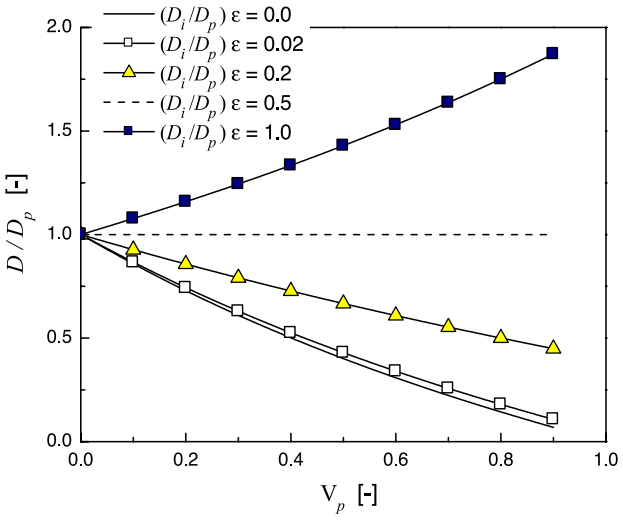

Fig. 6. Diffusivities of concretes and mortars from CSA model.

Table 1
Materials used for various test series

Specimen ID	w/b (−)	Type of cement	SCM (% by binder wt.)	
			Fly ash	Slag
NI-0	0.45	OPC	–	–
NI-PFA15	0.45	OPC	15.0	–
NI-PFA30	0.45	OPC	30.0	–
NI-PFA50	0.45	OPC	50.0	–
NI-BFS15	0.45	OPC	–	15.0
NI-BFS30	0.45	OPC	–	30.0
NI-BFS50	0.45	OPC	–	50.0
NV-0	0.45	SRPC	–	–
NV-PFA30	0.45	SRPC	30.0	–
NV-BFS30	0.45	SRPC	–	30.0
LI-0	0.55	OPC	–	–
HI-0	0.35	OPC	–	–
HI-PFA30	0.35	OPC	30.0	–
HI-BFS30	0.35	OPC	–	30.0

3. Tests for diffusivity measurement

To validate the model proposed in the present study, experimental measurements for the diffusion coefficients of concrete and mortar are carried out for various mixtures. The experimental details are as follows.

3.1. Materials and mixture proportions

The materials used and the mixture proportions for various test series are summarized in Tables 1 and 2,

Table 2
Mixture proportions

(a) Mixture proportions of concrete

Series	w/b	Binder (kg/m^3)	Water (kg/m^3)	Sand (kg/m^3)	Gravel (kg/m^3)	HRWRA† (kg/m^3)
L	0.55	316	174	749	1034	–
N	0.45	387	174	690	1035	1.94
H	0.35	497	174	621	1013	3.98

(b) Mixture proportions of mortar

Series	w/b	Binder (kg)	Water (kg)	Sand (kg)
L	0.55	1	0.55	2.37
N	0.45	1	0.45	1.78
H	0.35	1	0.35	1.25

† High-range water-reducing admixture.

Table 3
Oxide and compound composition of cement and SCM

Oxides/ compounds	Composition (wt.%)			
	OPC	SRPC	Fly ash	Blast–furnace slag
CaO	61.20	62.03	3.89	43.34
SiO_2	22.00	22.11	59.74	33.86
Al_2O_3	6.20	4.20	23.60	14.67
Fe_2O_3	3.20	4.27	6.07	0.32
MgO	2.80	2.87	0.95	5.95
K_2O	1.10	0.72	0.96	0.61
Na_2O	0.10	0.09	0.49	0.19
SO_3	2.00	2.03	0.40	0.12
LOI	1.40	1.70	3.90	0.67
Σ	100.00	100.02	100.00	99.73
C_3S	30.0	44.4	–	–
C_2S	40.5	29.9	–	–
C_3A	11.0	3.9	–	–
C_4AF	9.7	13.0	–	–
Gypsum	4.3	4.4	–	–
Σ	95.5	95.6		

respectively. The water-to-binder ratios of specimens are 0.35, 0.45 and 0.55, respectively. The ordinary Portland cement (ASTM Type I) and sulfate-resisting Portland cement (ASTM Type V) are used, and for supplementary cementitious materials (SCM), fly ash and blast-furnace slag are used up to 50% of total binder weight. The mineral and compound compositions of cement, fly ash and blast-furnace slag are listed in Table 3. The maximum size of aggregate was 25 mm and the particle size distributions of aggregates are shown in Fig. 7.

3.2. Test method and procedures

The electrical method proposed by Tang and Nilsson [26] is adopted for the measurement of the diffusivity of

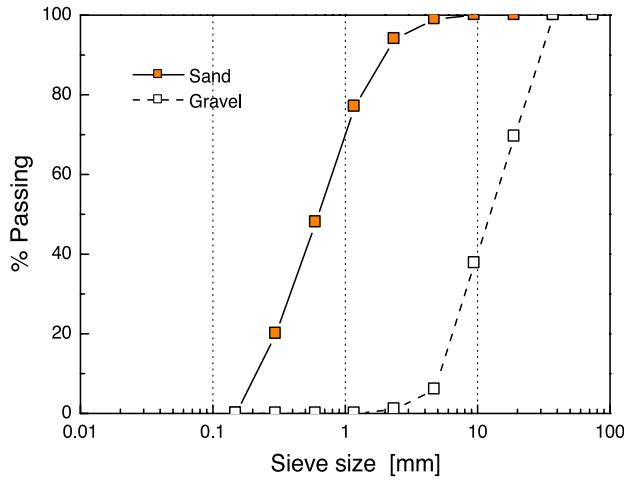

Fig. 7. Particle size distribution of aggregates.

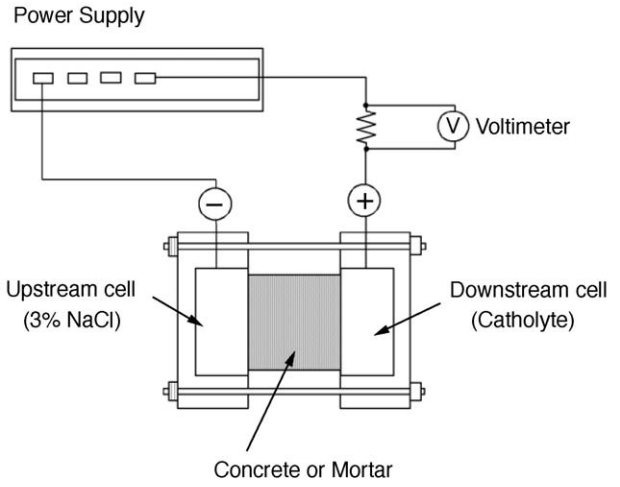

Fig. 8. Schematics of the test configuration (ASTM C 1202-97 [28]).

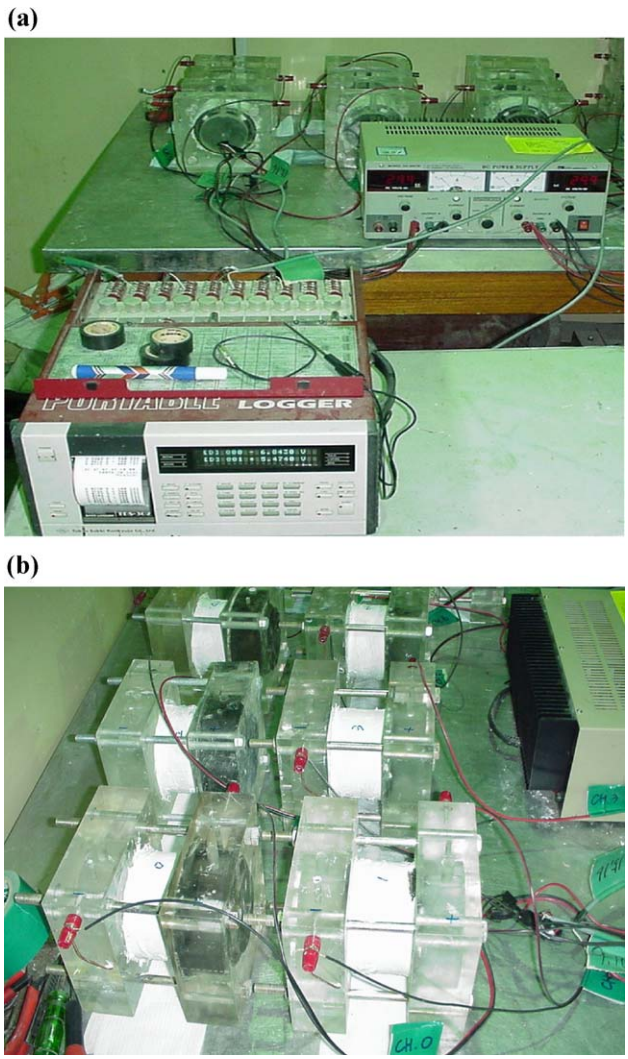

Fig. 9. Test set-up for diffusion coefficient measurement.

Table 4
Estimation of test duration [29]

Initial current, I_0 (mA)	Test duration (h)
$I_0 < 5$	168
$5 \le I_0 < 10$	96
$10 \le I_0 < 30$	48
$30 \le I_0 < 60$	24
$60 \le I_0 < 120$	8
$I_0 > 120$	4

concrete and mortar. This method is based on the non-steady-state migration test, and thus, requires relatively short test duration with fewer measurements. Nevertheless, it was reported that this method can provide sufficient accuracy [27].

The cylinder concrete and mortar specimens with 100 mm diameter and 200 mm length (ϕ 100 × 200 mm) were cast according to the mixture proportions in Table 2, and were cured in 20 °C water until the test. Before the test, a 50-mm-thick slice was taken from the center part of the cylinder specimen, the side of which was sealed with acrylic sealant. After the sealant is dry, the slice was placed in between the diffusion cells for the test. The diffusion cells and the test configuration are illustrated in Figs. 8 and 9 [see also the rapid chloride penetration test of ASTM C 1202-97 [28]]. The potential of 30 ± 0.2 V was applied between two diffusion cells during the test duration; the upstream cell (cathode) and the downstream cell (anode) were filled with 3% NaCl and 0.3 N NaOH solution, respectively. According to Tang [29], the test duration can be estimated from the initial current that is measured from the electric circuit at the beginning of the test (see Table 4).

The diffusivity of concrete is calculated by the following equation [29].

$$D_{\mathrm{nssm}} = \frac{RTL}{zFU}\frac{x_{\mathrm{d}} - \alpha\sqrt{x_{\mathrm{d}}}}{t_{\mathrm{d}}} \tag{10}$$

where D_{nssm} is the non-steady-state migration diffusion coefficients [m^2/s], x_{d} the penetration depth of chloride ions [m], t_{d} the test duration, and α is the test constant calculated by the following

$$\alpha = 2\sqrt{\frac{RTL}{zFU}}erf^{-1}\left(1 - \frac{2c_{\mathrm{d}}}{c_0}\right) \tag{11}$$

in which R is the gas constant (J/K mol) = 8.314 J/K mol, T the temperature of the upstream test solution (K), L the specimen thickness (m), z the ionic valence = 1 for chloride ions, F the Faraday constant = 96.5 kJ/V mol, U the applied potential (V) = 30 ± 0.2 V, and c_0 and c_{d} are the chloride concentrations in the upstream solution and at the chloride penetration front, respectively. After the test duration, the slice specimens were split into two pieces, and then the chloride penetration depth x_{d} was measured by the colorimetric method with 0.1 N silver chloride solution ($c_{\mathrm{d}} \approx 0.07$ N) (see Fig. 10).

4. Results and discussion

4.1. Non-steady-state migration diffusion coefficients

The measured non-steady-state migration (abbreviated as nssm) diffusion coefficients of all concrete and

Fig. 10. Measurement of chloride penetration depth.

mortar specimens are summarized in Table 5, and Fig. 11 shows the variation of D_{nssm} according to the compressive strengths, the water-to-binder ratios and the amount of mineral admixture. The values of the measured D_{nssm} are in the range of 1 to 15×10^{-12} m^2/s. In fact, there is some deviation between the two measurements made on each specimen. The deviation may come from the errors in the measurement of chloride penetration depth and the variation of test parameters, e.g., temperature (T), specimen length (L) and potential (U). However, this deviation is not too high, but reasonable if considering the conventional variation of concrete properties and the lack of accuracy in the conventional diffusion tests. Despite the deviation, one can find in Fig. 11b that the average diffusivities of two measurements are in good agreement with the data reported by Tang and Nilsson [27] and Tang [30]. Hence, only the average value is considered for the validation of the model in the following sections.

As expected, the diffusion coefficients of the specimens containing fly ash and slag are much lower than those of the Portland cement concrete specimens at the same levels of strength or water-to-binder ratio (see Fig. 11a–d). This is, of course, due to the finer pore structure of fly ash and slag cement pastes than that of Portland cement pastes. Feldman's MIP data [31] suggest that for mature pastes there is greater proportion of fine porosity in blend cement pastes than in Portland cement pastes. The effect of fly ash on the diffusion coefficients is more pronounced in Fig. 11c, which indicates that the diffusion coefficient decreases up to about 25% (of binder weight) addition of fly ash and then the diffusion coefficient again increases with the further addition of fly ash. This is probably due to the fact that when the amount of fly ash is larger than certain amount, the amount of $Ca(OH)_2$ is not enough for the pozzolanic reaction of fly ash. This will cause the smaller amount of the reaction products and thus the larger porosities; see the calculated porosities and the amounts of solid hydration products in Table 6, Section 4.2. In spite of the relatively larger porosity, however, the diffusion coefficients of 50% fly ash

Table 5
Measured non-steady-state diffusion coefficients

Specimen ID	1st			2nd			Average
	Age (days)	f_c' (MPa)	D_{nssm} ($\times 10^{-12}$ m^2/s)	Age (days)	f_c' (MPa)	D_{nssm} ($\times 10^{-12}$ m^2/s)	D_{nssm} ($\times 10^{-12}$ m^2/s)
(a) Concretes							
NI-O	156	40.3	7.714	174	47.4	5.401	6.557
NI-PFA15	156	31.8	3.538	170	48.4	3.543	3.540
NI-PFA30	156	52.6	3.006	170	50.0	2.115	2.561
NI-PFA50	153	26.0	4.873	192	43.6	2.171	3.522
NI-BFS15	151	–	6.297	172	48.2	5.233	5.765
NI-BFS30	164	46.9	6.723	172	49.6	4.111	5.417
NI-BFS50	151	41.7	2.625	190	53.0	2.646	2.636
NV-O	142	–	10.706	160	42.4	8.152	9.429
NV-PFA30	142	46.2	3.515	156	46.3	3.343	3.429
NV-BFS30	139	–	5.779	160	43.6	3.574	4.676
LI-O	139	43.6	21.154	160	33.7	10.262	15.708
HI-O	166	78.0	–	192	72.4	3.763	3.763
HI-PFA30	148	51.1	2.005	168	74.2	1.326	1.665
HI-BFS30	164	54.5	–	168	73.7	3.540	3.540
(b) Mortars							
NI-O	141	53.4	10.326	169	40.8	7.270	8.798
NI-PFA15	141	42.0	5.419	171	42.9	3.682	4.551
NI-PFA30	141	42.0	5.002	171	46.5	3.432	4.217
NI-PFA50	146	23.8	–	171	37.3	7.205	7.205
NI-BFS15	141	56.4	9.010	171	42.5	4.562	6.786
NI-BFS30	141	45.9	6.236	171	44.3	3.613	4.924
NI-BFS50	146	52.9	3.028	171	50.0	2.480	2.754
NV-O	145	53.9	14.160	168	37.1	9.709	11.935
NV-PFA30	145	46.5	5.673	168	40.0	4.406	5.040
NV-BFS30	145	44.1	6.429	168	39.2	4.551	5.490
LI-O	145	55.6	10.556	168	24.9	11.907	11.232
HI-O	145	64.7	–	172	67.6	5.400	5.400
HI-PFA30	145	60.3	3.669	170	70.0	2.143	2.906
HI-BFS30	145	71.2	–	172	69.3	2.919	2.919

concrete and mortar are still lower than the OPC pastes. This is because the pore structure of fly ash cement paste is more complex than that of Portland cement paste, and moreover, the solid phase diffusivity of the fly ash cement paste in Eq. (5) is much lower than that of the Portland cement paste. On the contrary, the diffusion coefficients of slag concrete decrease with increasing amount of slag (see Fig. 11d). Because slag has more CaO than fly ash, the porosities of specimens containing even up to 50% slag (of binder weight) do not increase relative to that of plain Portland cement concrete [see also Table 6]. The finer pore structure of slag cement concrete also reduces the diffusion coefficients.

4.2. Calculation of effective diffusivities from measured nssm diffusion coefficients

The nssm diffusion coefficients measured in this study cannot be directly compared to the effective diffusivities,

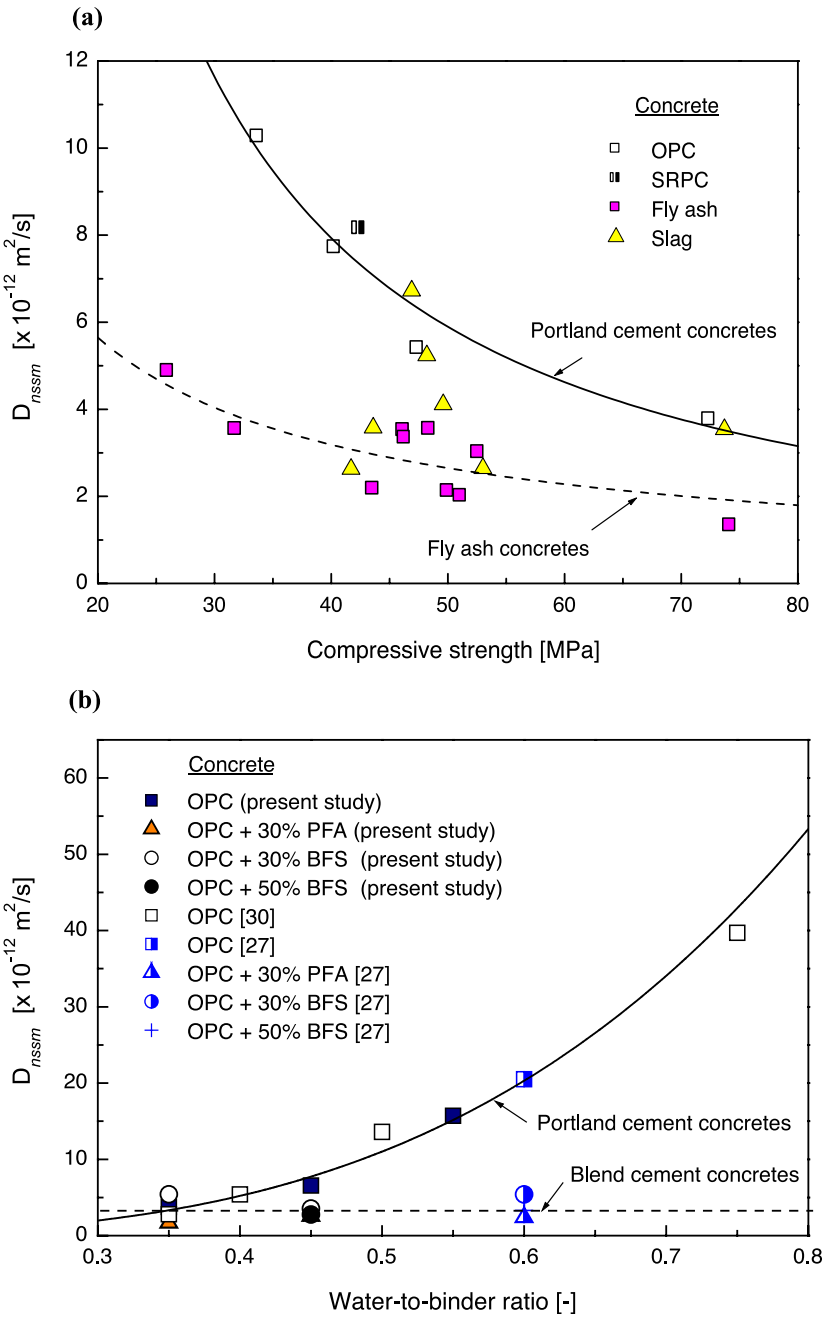

Fig. 11. Effect of strength, water-to-binder ratio, and amount of fly ash or slag on the measured non-steady-state migration diffusion coefficients.

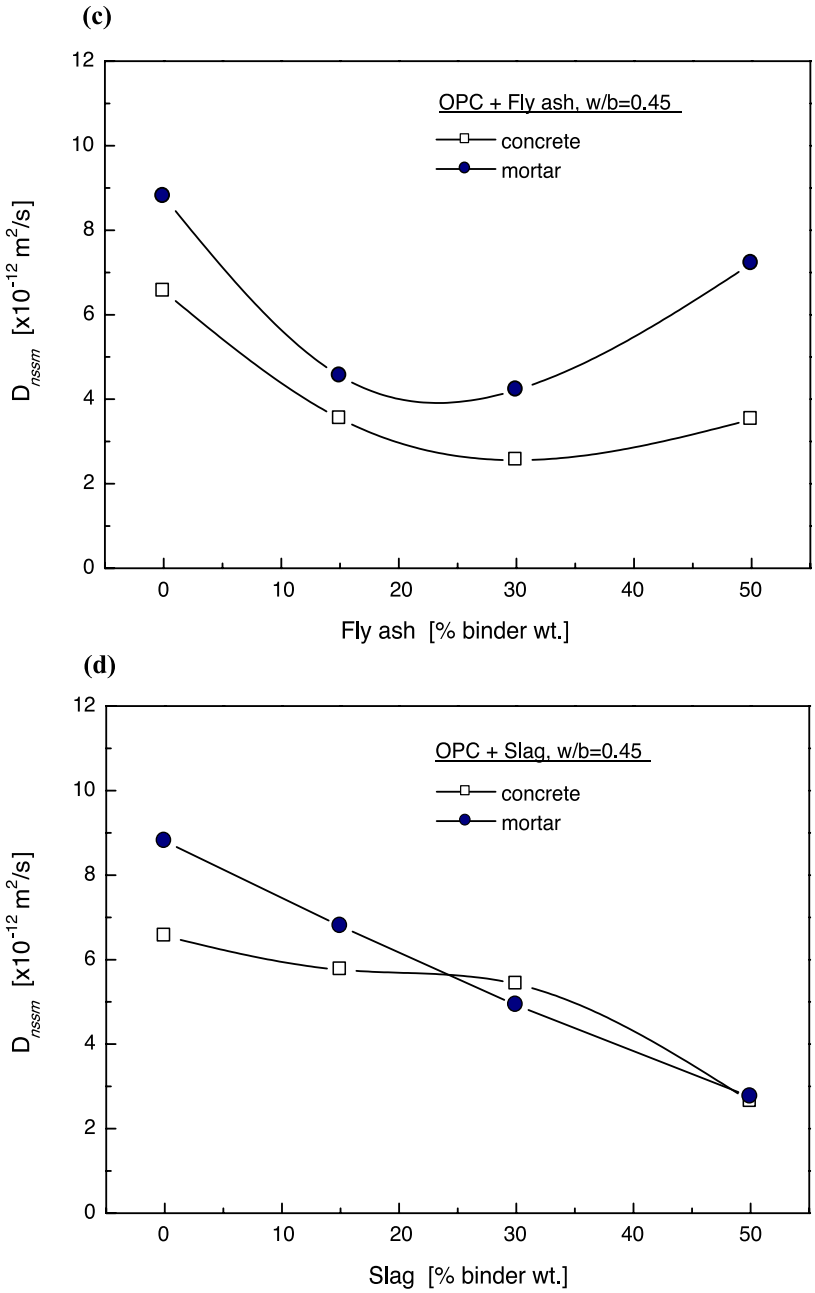

Fig. 11 (*continued*).

and hence need to be converted. According to Tang [30], the effective diffusivity can be obtained from the diffusion coefficients measured from the non-steady-state migration test by the following equation.

$$D = D_{\mathrm{nssm}}(\phi + K_{\mathrm{b}} W_{\mathrm{hyd}}) \tag{12}$$

where ϕ is the total porosity per total volume of concrete or mortar (−), K_{b} is the chloride binding constant during the migration test (−), and W_{hyd} is the weight of hydration products per unit volume of concrete (or mortar) (kg/m^3)[see Table 6]. The values of K_{b} are calculated based on the experimental data reported by Tang [32] and Delagrave et al. [33], and also shown in Table 6. The detailed calculation of K_{b} can be found in Ref. [30].

The capillary porosity ϕ_{cap}, total porosity ϕ and the weight of hydration products W_{hyd} are calculated by the stoichiometry of the cement hydration and the pozzolanic reactions [34,35]. This calculation is based on the ultimate

Table 6
Calculation of effective diffusivities from measured *nssm* diffusion coefficients

Specimen ID	D_{nssm} ($\times 10^{-12}$ m^2/s)		ϕ (−)		W_{hyd} (kg/m^3)		$K_b^{\dagger}$ ($\times 10^{-3}$)	D (measured, $\times 10^{-12}$ m^2/s)	
	Concrete	Mortar	Concrete	Mortar	Concrete	Mortar		Concrete	Mortar
NI-O	6.557	8.798	0.126	0.215	412.1	700.1	0.59	2.425	5.526
NI-PFA15	3.540	4.551	0.135	0.228	382.4	646.2	0.73	1.466	3.184
NI-PFA30	2.561	4.217	0.144	0.242	340.9	573.0	0.73	1.005	2.784
NI-PFA50	3.522	7.205	0.155	0.260	263.7	440.3	0.73	1.226	4.188
NI-BFS15	5.765	6.786	0.125	0.212	406.4	689.7	0.61	2.160	4.314
NI-BFS30	5.417	4.924	0.124	0.210	400.7	679.3	0.61	2.004	3.088
NI-BFS50	2.636	2.754	0.122	0.207	393.1	665.5	0.75	1.097	1.941
NV-O	9.429	11.94	0.139	0.236	395.5	671.9	0.55	3.350	7.203
NV-PFA30	3.429	5.040	0.150	0.253	333.5	560.7	0.59	1.191	2.943
NV-BFS30	4.676	5.490	0.133	0.225	391.2	663.3	0.59	1.702	3.388
LI-O	15.71	11.23	0.134	0.227	364.0	617.7	0.59	5.475	6.644
HI-O	3.763	5.400	0.117	0.196	470.1	785.8	0.59	1.485	3.563
HI-PFA30	1.665	2.906	0.135	0.223	401.9	663.2	0.73	0.714	2.056
HI-BFS30	3.540	2.919	0.112	0.186	472.7	788.1	0.61	1.422	1.955

† Assumed based on Tang's [32] and Delagrave et al., [33] experimental data.

degree of cement hydration (α_c), which is empirically given by

$$\alpha_c = 1 - 3.15\exp(w/b) \quad (13)$$

in which w/b is the water-to-binder ratio [36]. Since the actual calculation requires quite complicated procedures, the detailed calculations are not described here, but can be found in Ref. [13]. Fig. 12 indicates that the porosities of cement pastes with or without pozzolans and slag obtained by such calculation agree well with the experimental data measured by the mercury intrusion porosimetry (MIP)[37,38].

Finally, the effective diffusivities are obtained as shown in Table 6.

4.3. Prediction of effective diffusivities

With the model proposed in Eq. (9), the effective diffusivities of concretes and mortars can be calculated as follows.

4.3.1. Calculation of effective diffusivities of cement paste

For the prediction of the effective diffusivities, the parameters for Δ_a in Eq. (9) are to be determined first. For

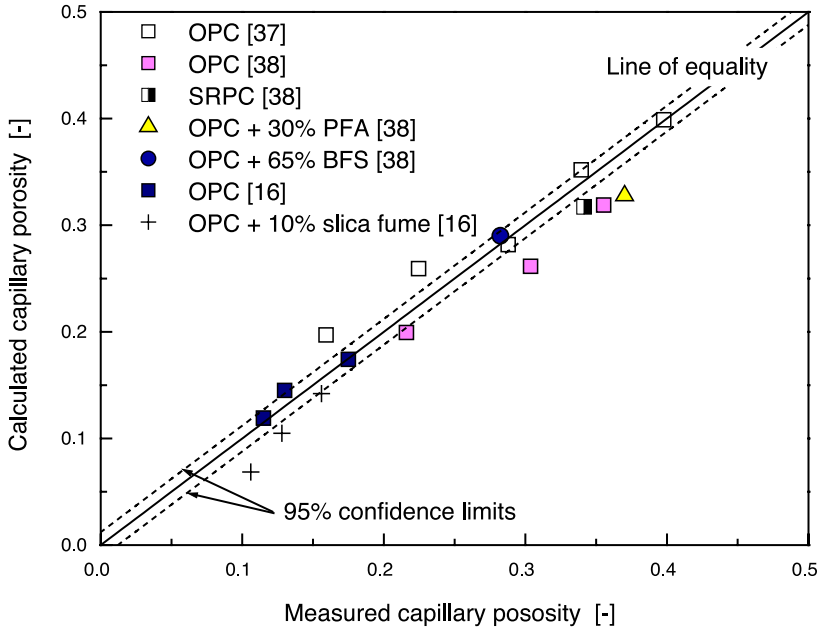

Fig. 12. Comparison of calculated and measured capillary porosities.

this, the value of ε may be approximated by considering the mean radius of aggregate particles. The mean radius of the fine aggregates used in this study is found to be approximately 1.0 mm, and that of the coarse aggregates is approximately 15.6 mm (see Fig. 7). In addition, the thickness of ITZ is assumed here approximately 20 μm based on Scrivener and Nemati's [39] observation. Then, the values of ε are determined as ≈ 0.02 for mortar, and ≈ 0.002 for concrete.

The comparison of Eqs. (7a) and (7b) with Delagrave et al.'s [40] experimental data gives the value of $D_i/D_p \approx 6$ to 10 (see Fig. 13). Breton et al. [41] and Bourdette et al. [42] argue that the effective diffusion coefficient of ITZ is 6 to 12 times greater than that of bulk cement paste. These two results coincide. Also, the report of Shane et al. [43] that the D_i/D_p varies from 2 to 7 with degree of hydration and for mature concrete with the degree of hydration of 0.5–0.8, $D_i/D_p \approx 7$. Summarizing the above results, D_i/D_p is assumed 7.

With the values assumed in the above, the effective diffusivities of cement pastes can then be calculated from the measured effective diffusivities of concretes and mortars which are denoted by D_p (measured) in Table 6. The diffusivities of cement pastes obtained from such calculation indicate that $D_s/D_0 = 1.0 - 2.0 \times 10^{-4}$ and $n = 2.7$ are good approximations for Portland cement pastes (see Table 7a and Fig. 14a). On the contrary, $n = 4.5$ seems more valid and $D_s/D_0 \approx 0.5 - 2.0 \times 10^{-4}$ for slag cement pastes. For fly ash cement pastes, n also equals to 4.5 but D_s/D_0 varies from 0.1 to 5.0×10^{-5} according to the amount of fly ash. These values of n are same with those of the silica fume pastes found in the previous section, and the D_s/D_0 values are very similar as well. With these values of n and D_s/D_0, the diffusivities of cement pastes are also calculated from Eqs. (6a) and (6b) (see Table 7b). As shown in Fig. 14b, the diffusivities of cement pastes determined from two different procedures exhibit good correlation.

In Fig. 14a, it is also notable that the values of D_s/D_0 for the specimens with the lower degree of hydration (i.e., higher water-to-binder ratio in this case [see Eq. (13)]) are rather lower, which means that the degree of hydration also affects D_s/D_0 to some extent. It can be deduced that the C-S-H proportions in total solid phase will influence the D_s/D_0 because of existence of gel pores in the C-S-H. Thus, D_s/D_0 will increases with the increasing of the degree of hydration, especially in early ages. This may be why there are discrepancies between the diffusivities of early-age cement pastes and Eqs. (6a) and (6b) in Fig. 4. This suggests that further study is needed to apply the present model to very early-age concrete. Nevertheless, the variation of D_s/D_0 with hydration may be negligible for mature cement pastes.

4.3.2. Calculation of the effective diffusivities of concrete and mortar

Using the model parameters that were determined in the above, the effective diffusivities of concretes and mortars were calculated and summarized in Table 7c. In this calculation, D_i/D_p is calculated by Eqs. (6a) and (6b)

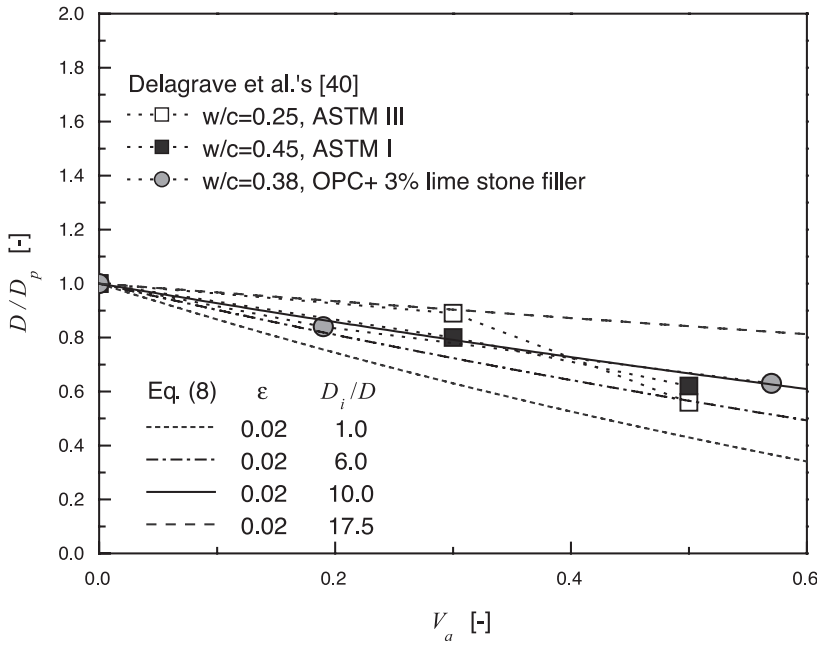

Fig. 13. Comparison of Eq. (8) and the experimental data of Delagrave et al. [40] on the diffusivities of mortars according to aggregate volume fractions.

Table 7
Prediction of the effective diffusivities of concrete and mortar

(a) Diffusivities of cement pastes calculated from measured diffusivities of concretes and mortars

Specimen ID	D_i/D_p (−)	ε (−)		V_a(−)		D_p(calculated) ($\times 10^{-12}$ m^2/s)		
		Concrete	Mortar	Concrete	Mortar	From D_{con}[a]	From D_{mor}[a]	Average
NI-O	7	0.002	0.02	0.6846	0.4642	9.368	8.965	9.166
NI-PFA15	7	0.002	0.02	0.6794	0.4582	5.572	5.128	5.350
NI-PFA30	7	0.002	0.02	0.6743	0.4524	3.762	4.454	4.108
NI-PFA50	7	0.002	0.02	0.6675	0.4448	4.492	6.641	5.567
NI-BFS15	7	0.002	0.02	0.6836	0.463	8.318	6.989	7.654
NI-BFS30	7	0.002	0.02	0.6794	0.4582	7.618	4.974	6.296
NI-BFS50	7	0.002	0.02	0.6825	0.4618	4.211	3.139	3.675
NV-O	7	0.002	0.02	0.6811	0.4601	12.800	11.629	12.215
NV-PFA30	7	0.002	0.02	0.6743	0.4524	4.457	4.709	4.583
NV-BFS30	7	0.002	0.02	0.6825	0.4618	6.534	5.481	6.007
LI-O	7	0.002	0.02	0.7084	0.5052	22.850	11.313 (d[b])	22.850
HI-O	7	0.002	0.02	0.6480	0.4115	5.139	5.440	5.290
HI-PFA30	7	0.002	0.02	0.7026	0.4853	2.923	3.419	3.171
HI-BFS30	7	0.002	0.02	0.6454	0.4088	4.884	2.976	3.930

(b) Diffusivities of cement pastes calculated by Eqs. (6a) and (6b)

Specimen ID	D_s/D_0 ($\times 10^{-4}$)	n (−)	ϕ_c (−)	ϕ_{cap} (−)	D_p/D_0[c] ($\times 10^{-3}$)	D_p (by Eqs. (6a) and (6b)) ($\times 10^{-12}$ m^2/s)
NI-O	1.0	2.7	0.18	0.225	4.357	8.853
NI-PFA15	0.5	4.5	0.18	0.256	2.831	4.883
NI-PFA30	0.1	4.5	0.18	0.279	1.709	3.447
NI-PFA50	0.01	4.5	0.18	0.352	3.095	5.896
NI-BFS15	2.0	4.5	0.18	0.224	2.511	6.666
NI-BFS30	2.0	4.5	0.18	0.222	2.443	6.512
NI-BFS50	0.5	4.5	0.18	0.219	2.345	2.871
NV-O	1	2.7	0.18	0.260	7.660	15.57
NV-PFA30	0.1	4.5	0.18	0.297	2.323	4.534
NV-BFS30	1.0	4.5	0.18	0.247	3.437	6.090
LI-O	1.0	2.7	0.18	0.286	11.17	22.70
HI-O	2.0	2.7	0.18	0.161	1.351	4.304
HI-PFA30	0.5	4.5	0.18	0.214	0.468	2.693
HI-BFS30	2.0	4.5	0.18	0.141	0.775	2.446

(c) Diffusivities of concretes and mortars

Specimen ID	ϕ_{ITZ}[d] (−)	D_i/D_p (−)	ε (−)		V_a (−)		D (calculated, $\times 10^{-12}$ m^2/s)	
			Concrete	Mortar	Concrete	Mortar	Concrete	Mortar
NI-O	0.338	4.986	0.002	0.02	0.685	0.464	2.231	5.014
NI-PFA15	0.384	5.115	0.002	0.02	0.679	0.458	1.250	2.781
NI-PFA30	0.419	8.255	0.002	0.02	0.674	0.452	0.923	2.163
NI-PFA50	0.527	11.97	0.002	0.02	0.668	0.445	1.681	4.216
NI-BFS15	0.335	4.050	0.002	0.02	0.684	0.463	1.649	3.512
NI-BFS30	0.332	4.023	0.002	0.02	0.679	0.458	1.633	3.453
NI-BFS50	0.328	3.981	0.002	0.02	0.683	0.462	0.722	1.583
NV-O	0.391	4.985	0.002	0.02	0.681	0.460	3.967	8.867
NV-PFA30	0.445	8.277	0.002	0.02	0.674	0.452	1.217	2.868
NV-BFS30	0.370	4.352	0.002	0.02	0.683	0.462	1.529	3.338
LI-O	0.429	4.901	0.002	0.02	0.708	0.505	5.274	12.07
HI-O	0.241	4.169	0.002	0.02	0.648	0.412	1.194	2.469
HI-PFA30	0.321	7.513	0.002	0.02	0.703	0.485	0.632	1.428
HI-BFS30	0.212	2.749	0.002	0.02	0.645	0.409	0.675	1.344

[a] D_{con} and D_{mor} are the effective diffusivities D (measured) of concrete and mortar in Table 6, respectively.
[b] Discarded.
[c] At 25 °C ($D_0 = 2.032 \times 10^{-9}$ m^2/s).
[d] $\phi_{ITZ} \approx 1.5\ \phi_{cap}$ is assumed, according to Bourdette et al. [42].

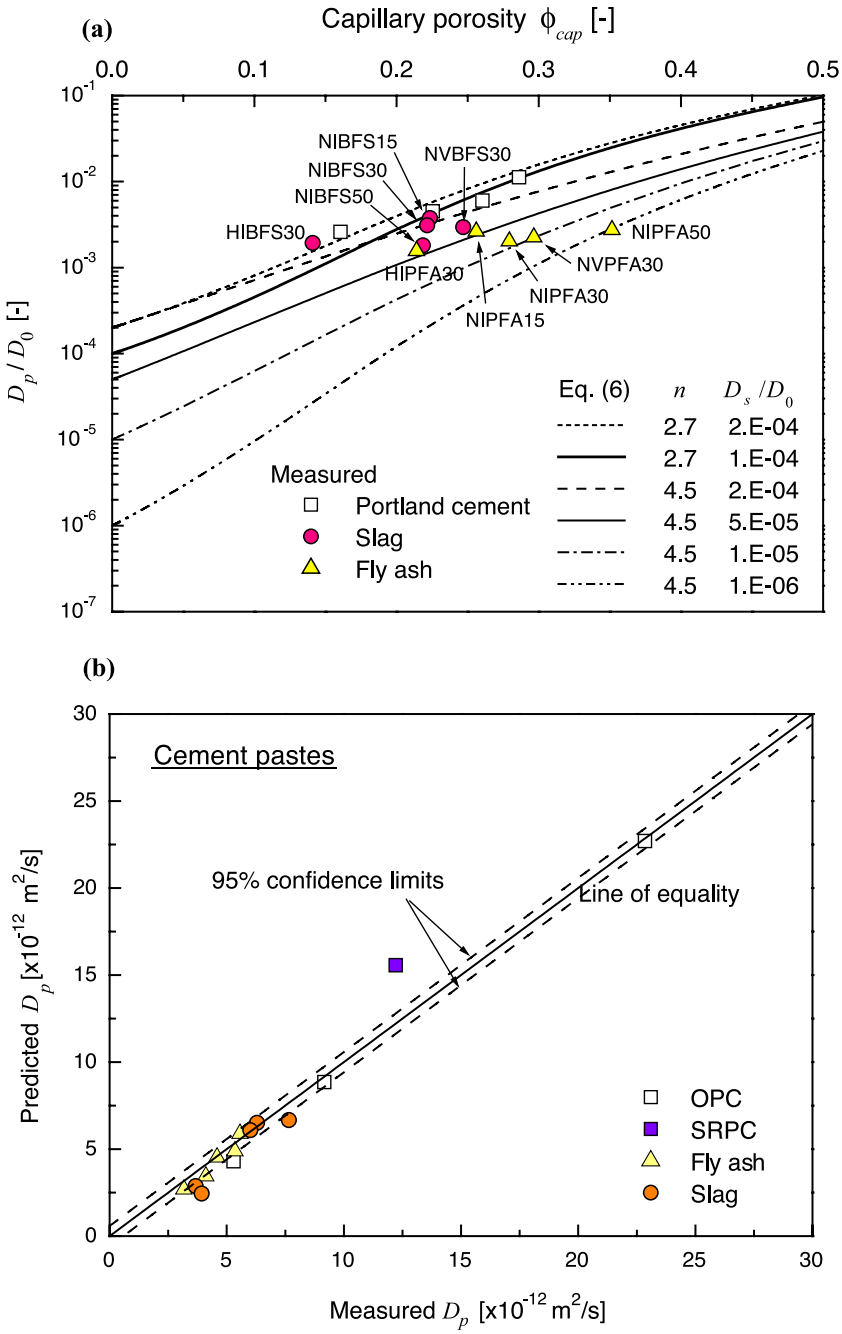

Fig. 14. Comparison of predicted and measured diffusivities of cement pastes.

assuming $\phi_{ITZ} \approx 1.5\phi_{cap}$ after Bourdette et al. [42]. As shown in Table 7c, it varies from 2 to 12 but is mostly in the range of 4 to 8, which coincides with the calculation of Shane et al. [43].

Fig. 15 shows that the predicted diffusivities are in reasonable agreement with the measured ones for both concretes and mortars. The accuracy of the model predictions is dependent on the model parameters as well as the accuracy of the calculated porosities. The most sensitive parameter is probably the solid phase diffusivity of the paste because it varies generally in very wide range relative to other parameters. In this study, the model parameters such as the solid phase diffusivity and percolation exponent are approximately determined based on limited experimental data. However, because each parameter in the present model has its own physical meaning, it is expected that they can be more accurately determined if relevant experimental data are available. For example, accurate diffusivity data for cement pastes with much lower porosities can yield a

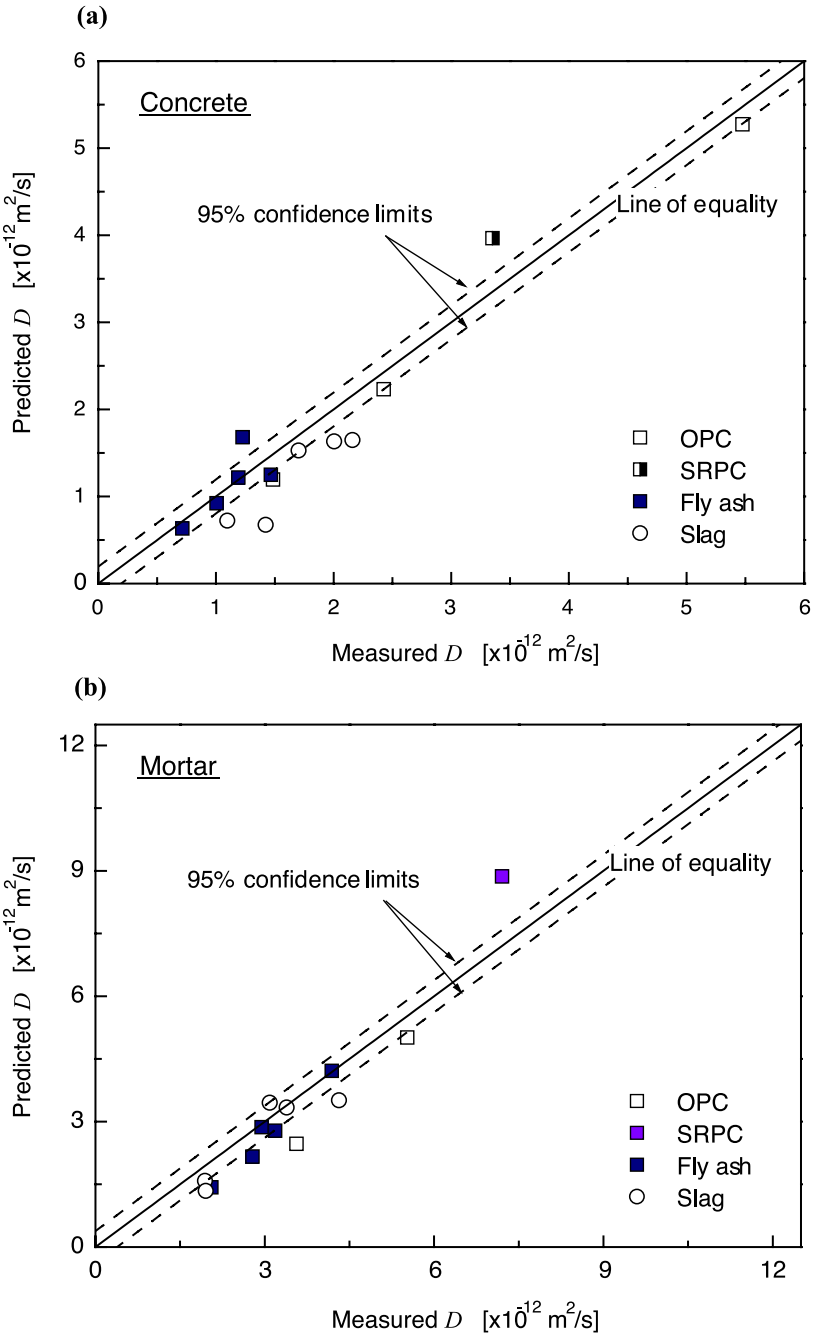

Fig. 15. Comparison of predicted and measured diffusivities of concrete and mortar.

higher reliability in determining the solid phase diffusivity D_s.

5. Conclusion

The purpose of this study is to propose a simple analytic model to determine the diffusivity of concrete and mortar. To this end, the relationship between the diffusivity and the microstructure of concrete has been considered. The microstructure considered here includes the interfacial transition zone (ITZ) between the aggregate particles and the bulk cement pastes as well as the microstructure of the bulk cement paste itself. To derive the effective diffusivity of cement paste, the general effective media (GEM) equation, which was originally developed for the electrical conductivity of composites, has been adopted in this study. The effective diffusivity of concrete is also derived by employing the composite spheres assemblage (CSA) model, which considers the diffusivities of both ITZ and cement paste.

The main variables of the model are the capillary porosity and aggregate volume fraction, and the major parameters include the percolation exponent and percolation threshold, which represent the tortuosity and constrictivity of pore structure, the solid phase diffusivity which accounts for the diffusion through the hydrated solid phase, and the interfacial properties such as thickness and diffusivity of transition zone.

To validate the model proposed in the present study, the measurement of the diffusivities has been carried out on a number of series of concrete and mortar specimens with the major test variables of the compressive strength, water-to-binder ratio, and the addition of mineral admixtures. The comparison of the proposed theory with the test data shows good agreement. The parameters of the proposed model have been also determined from the test data.

The proposed model is simple, yet realistic which can be used for reasonable durability design of concrete structures.

Acknowledgements

The support from the National Research Laboratory Program of Korea to this laboratory is gratefully acknowledged. The support from the Ministry of Construction and Transportation (MOCT) of Korea is also appreciated.

References

[1] P.K. Mehta, P.J.M. Monteiro, Concrete: Structure, Properties, and Materials, 2nd ed., Prentice Hall, Englewood Cliffs, NJ, 1993.
[2] E.J. Garboczi, Permeability, diffusivity, and microstructural parameters. A critical review, Cem. Concr. Res. 20 (4) (1990) 591–601.
[3] A. Atkinson, A.K. Nickerson, The diffusion of ions through water-saturated cement, J. Mater. Sci. 19 (1984) 3068–3078.
[4] J.D. Shane, T.O. Mason, H.M. Jennings, Conductivity and microstructure of the interfacial transition zone measured by impedance spectroscopy, in: M.G. Alexander, G. Arliguie, G. Ballivy, A. Bentur, J. Marchand (Eds.), Engineering and Transport Properties of the Interfacial Transition Zone in Cementitious Composites, E & FN Spon, London, 1999, pp. 173–203.
[5] J. van Brakel, P.M. Heertjes, Analysis of diffusion in macroporous media in terms of a porosity, a tortuosity and a constrictivity factor, Int. J. Heat Mass Transfer 17 (1974) 1092–1103.
[6] W.J. Moore, Physical Chemistry, 4th ed., Prentice-Hall Englewood Cliffs, New Jersey, 1972.
[7] G.E. Archie, The electrical resistivity log as an aid in determining some reservoir characteristics, Trans. AIME 156 (1942) 54–67.
[8] D.S. McLachlan, M. Blaszkiewicz, R.E. Newnham, Electrical resistivity of composites, J. Am. Ceram. Soc. 73 (1990) 2187–2203.
[9] D.P. Bentz, E.J. Garboczi, Percolation of phases in a three-dimensional cement paste microstructural model, Cem. Concr. Res. 21 (2–3) (1991) 325–344.
[10] H. Scher, R. Zallen, Critical density in percolation processes, J. Chem. Phys. 53 (1970) 3759–3761.
[11] D.P. Bentz, O.M. Jensen, A.M. Coats, F.P. Glasser, Influence of silica fume on diffusivity in cement-based materials, I. Experimental and computer modeling studies on cement pastes, Cem. Concr. Res. 30 (2000) 953–962.
[12] E.J. Garboczi, D.P. Bentz, Computer simulation of the diffusivity of cement-based materials, J. Mater. Sci. 27 (1992) 2083–2092.
[13] S.Y. Jang, Modeling of Chloride Transport and Carbonation in Concrete and Prediction of Service Life of Concrete Structures Considering Corrosion of Steel Reinforcements, PhD thesis, Dept. of Civil Engineering, Seoul National University, Seoul, 2003.
[14] B.J. Christensen, R.T. Coverdale, R.A. Olson, S.J. Ford, E.J. Garboczi, H.M. Jennings, T.O. Mason, Impedance spectroscopy of hydrating cement-based materials: Measurement, interpretation and application, J. Am. Ceram. Soc. 77 (11) (1994) 2789–2804.
[15] P.J. Tumidajski, A.S. Schumacher, S. Peron, P. Gu, J.J. Beaudoin, On the relationship between porosity and electrical resistivity of cementitious system, Cem. Concr. Res. 26 (1996) 539–544.
[16] M.-H. Zhang, O.E. Gjørv, Effect of silica fume on pore structure and chloride diffusivity of low porosity cement pastes, Cem. Concr. Res. 21 (1991) 1006–1014.
[17] A. Delagrave, J. Marchand, M. Pigeon, Influence of microstructure on the tritiated water diffusivity of mortars, Adv. Cem. Based Mater. 7 (1998) 60–65.
[18] O.M. Jensen, P.F. Hansen, A.M. Coats, F.P. Glasser, Chloride ingress in cement paste and mortar, Cem. Concr. Res. 29 (1996) 1497–1504.
[19] R.F. Feldman, H. Cheng-yi, Properties of Portland cement–silica fume pastes. I. Porosity and surface properties, Cem. Concr. Res. 15 (5) (1985) 765–774.
[20] D.N. Winslow, M.D. Cohen, D.P. Bentz, K.A. Snyder, E.J. Garboczi, Percolation and pore structure in mortars and concrete, Cem. Concr. Res. 24 (1) (1994) 25–37.
[21] E.J. Garboczi, D.P. Bentz, Multiscale analytical/numerical theory of the diffusivity of concrete, Adv. Cem. Based Mater. 8 (1998) 77–88.
[22] Z. Hashin, Thin interphase/imperfect interface in conduction, J. Appl. Phys. 89 (4) (2001) 2261–2267.
[23] Z. Hashin, S. Shtrikman, A variational approach to the theory of the effective magnetic permeability of multiphase materials, J. Appl. Phys. 33 (10) (1962) 3125–3131.
[24] Z. Hashin, P.J.M. Monteiro, An inverse method to determine the elastic properties of the interface between the aggregate and cement paste, Cem. Concr. Res. 32 (2002) 1291–1300.
[25] Handbook of Chemistry and Physics, 81st ed., CRC Press, Washington, DC, 2000–2001.
[26] L. Tang, L.-O. Nilsson, Rapid determination of chloride diffusivity of concrete by applying an electric field, ACI Mater. J. 49 (1) (1992) 49–53.
[27] L. Tang, L.-O. Nilsson, A rapid method for measuring chloride diffusivity by using an electric field, in: L.-O. Nilsson (Ed.), Chloride Penetration into Concrete Structures–Nordic Miniseminar, Division of Building Materials, Chalmers University of Technology, Göteborg, Sweden, 1993, pp. 26–35, Publication P-93:1.
[28] ASTM C 1202-97, Standard test method for electrical indication of concrete ability to resist chloride ion penetration. Annual Book of ASTM Standards. v. 04.02, 1997.
[29] L. Tang, Electrically accelerated methods for determining chloride in concrete, Mag. Concr. Res. 48 (176) (1996) 173–179.
[30] L. Tang, On chloride diffusion coefficients obtained by using electrically accelerated methods, in: N.-O. Nilsson, J.P. Ollivier (Eds.), Proceedings of the RILEM International Workshop on Chloride Penetration into Concrete (Oct. 15–18, 1995, St. Rémy-lès-Chevreuse, France), RILEM publications, Cachan, 1995, pp. 126–134.
[31] R.F. Feldman, in: S. Diamond (Ed.), Effects of Fly Ash in Cement and Concrete, Materials Research Society, University Park, PA, 1981, p. 124.
[32] L. Tang, Chloride Transport in Concrete, Licentiate thesis, Publication P-96:6, Division of Building Materials, Chalmers University of Technology, Göteborg, Sweden, 1996.
[33] A. Delagrave, J. Marchand, J.-P. Ollivier, S. Julien, K. Hazrati, Chloride binding capacities of various hydrated cement paste systems, Adv. Cem. Based Mater. 6 (1997) 28–35.
[34] P.D. Tennis, H.M. Jennings, A model for two types of calcium silicate hydrate in the microstructure of Portland cement pastes, Cem. Concr. Res. 30 (2000) 855–863.

[35] V.G. Papadakis, C.G. Vayenas, M.N. Fardis, Hydration and carbonation of pozzolanic cements, ACI Mater. J. 89 (1992) 119–130.
[36] V. Waller, F. DeLarrard, P. Roussel, Modelling the temperature rise in massive HPC structures (Paper 170), 4th International Symposium on Utilization of High-Strength/High-Performance Concrete, Presses de l'ENPC, Paris, 1996, pp. 415–421.
[37] R.A. Cook, K.C. Hover, Mercury porosimetry of hardened cement pastes, Cem. Concr. Res. 29 (1999) 933–943.
[38] C.L. Page, N.R. Short, A. El Tarras, Diffusion of chloride ions in hardened cement paste, Cem. Concr. Res. 11 (3) (1981) 395–406.
[39] K.L. Scrivener, K.M. Nemati, The percolation of pore space in the cement paste/aggregate interfacial zone of concrete, Cem. Concr. Res. 26 (1) (1996) 35–40.
[40] A. Delagrave, J.P. Bigas, J.-P. Ollivier, J. Marchand, M. Pigeon, Influence of interfacial zone on the chloride diffusivity of mortars, Adv. Cem. Based Mater. 5 (1997) 86–91.
[41] D. Breton, J.-P. Ollivier, G. Ballivy, Diffusivity of chloride ions in the transition zone between cement paste and granite, in: J.C. Maso (Ed.), Interfaces between Cementitious Composites, E & FN Spon, London, 1992, pp. 279–288.
[42] B. Bourdette, E. Ringot, J.-P. Ollivier, Modeling of the transition zone porosity, Cem. Concr. Res. 25 (4) (1995) 741–751.
[43] J.D. Shane, T.O. Mason, H.M. Jennings, Effect of the interfacial transition zone on the conductivity of Portland cement mortars, J. Am. Ceram. Soc. 83 (5) (2000) 1137–1144.